Supernova – the explosive death of an entire star –*

currently active supernovae are given at

http://www.rochesterastronomy.org/supernova.html

* *Usually, you only die once*

Basic spectroscopic classification of supernovae

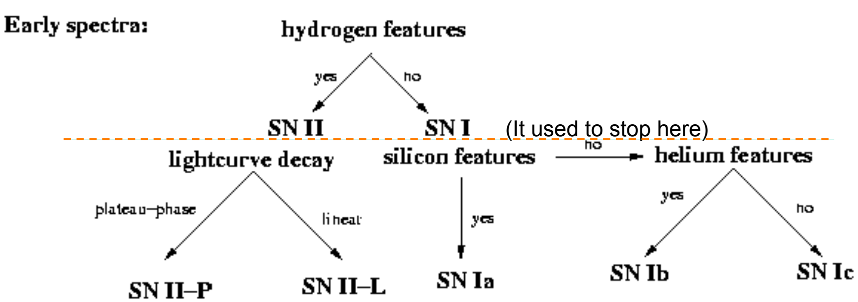

Also II b, II n, Ic – High vel, I-pec, UL-SN, etc.

Observational Properties: Type Ia supernovae

- The "classical" SN I; no hydrogen; strong Si II 6347, 6371 line
- Maximum light spectrum dominated by P-Cygni features of Si II, S II, Ca II, O I, Fe II and Fe III
- Nebular spectrum at late times dominated by Fe II, III, Co II, III
- Found in all kinds of galaxies, elliptical to spiral, some mild evidence for a association with spiral arms
- Prototypes 1972E (Kirshner and Kwan 1974) and SN 1981B (Branch et al 1981)
- Brightest kind of common supernova, though briefer. Higher average velocities. $M_{bol} \sim -19.3$
- Assumed due to an old stellar population. Favored theoretical model is an accreting CO white dwarf that ignites a thermonuclear runaway and is completely disrupted.

Spectra of SN Ia near maximum are very similar from event to event

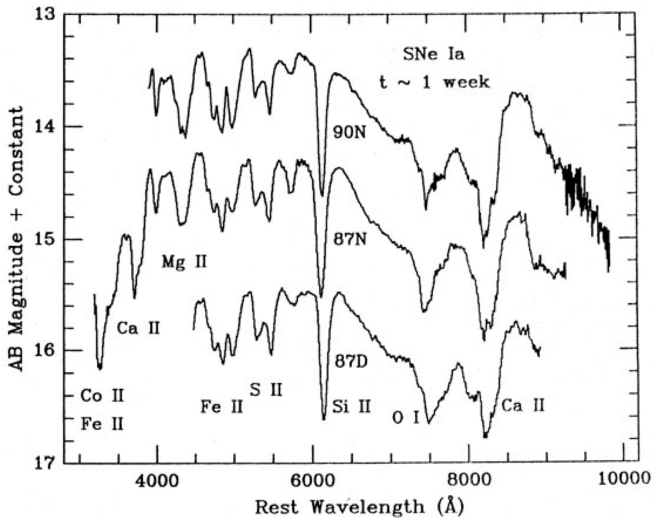

Spectra of three Type Ia supernovae near peak light – courtesy Alex Filippenko

	Possible Type Ia Supernovae in Our Galaxy		
	SN	D(kpc)	m_V
	185	1.2+-0.2	-8+-2
	1006	1.4+-0.3	-9+-1
Tycho	1572	2.5+-0.5	-4.0+-0.3
Kepler	1604	4.2+-0.8	-4.3+-0.3

Expected rate in the Milky Way Galaxy about 1 every 200 years, but dozens are found in other galaxies every year. About one SN Ia occurs per decade closer than about 5 Mpc.

2011fe a SN Ia reached appaent magnitude 9.9, 21 Mly. 72e was closer

Low Redshift Type Ia Template Lightcurves

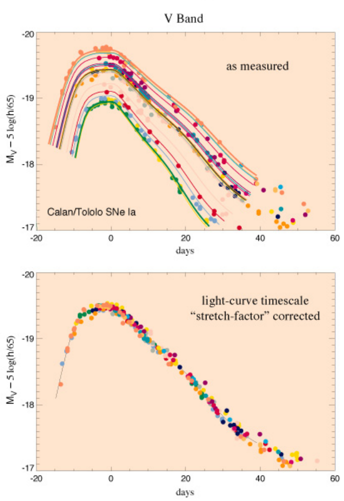

The Phillips Relation
(post 1993)

Broader = Brighter

Can be used to compensate for the variation in observed SN Ia light curves to give a "calibrated standard candle".

Note that this makes the supernova luminosity at peak a function of a single parameter – e.g., the width.

Properties: Type Ib/c supernovae

- Lack hydrogen, but also lack the Si II $\lambda\lambda$6355 feature that typifies SN Ia.
- SN Ib have strong features due to He I at 5876, 6678, 7065 and 10830 A. SN Ic lack these helium features, at least the 5876 A line. Some people think there is a continuum of properties between SN Ib and SN Ic
- Found in spiral and irregular galaxies. Found in spiral arms and star forming regions. Not found in ellipticals. Associated with star formation
- Often strong radio sources
- Fainter at peak than SN Ia by about 1.5 magnitudes. Otherwise similar light curve.
- Only supernovae definitely associated with gamma-ray bursts so far are Type Ic
- Cannot have high mass in the common case. Probably come from binaries

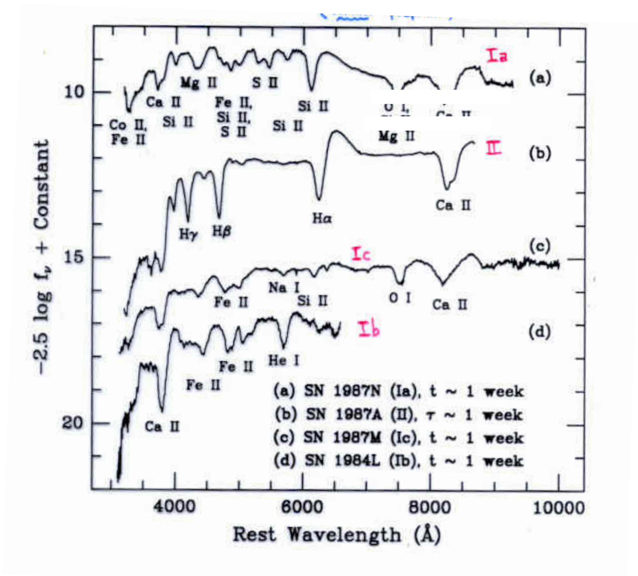

Filippenko, (1996), *Ann. Rev. Astron. Ap*

Properties: Type II supernovae

- Have strong Balmer lines – H_α, H_β, H_γ - in peak light and late time spectra. Also show lines of Fe II, Na I, Ca II, and, if the supernova is discovered early enough, He I.
- Clearly come from massive stars. Found in star forming regions of spiral and irregular galaxies. Not found in ellipticals. Several dozen presupernova stars have been identified: SN 1987A = B3 supergiant; SN 1993J = G8 supergiant (Aldering et al 1994)
- Usually fainter than Type I, but highly variable in brightness (presumably depending on hydrogen envelope mass and radius and the explosion energy). Typically lower speed than Type Ia. Last longer.
- Come in at least two varieties (in addition to 87A) – Type II-p or "plateau" and Type II-L or "linear". There may also be Type II-b supernovae which have only a trace amount of hydrogen left on what would otherwise have been a Type Ib/c (e.g., SN 1993J)
- Strong radio sources, and at least occasionally emit neutrino bursts

<u>Typical Type II-p on the Plateau</u>

Filippenko (1990)

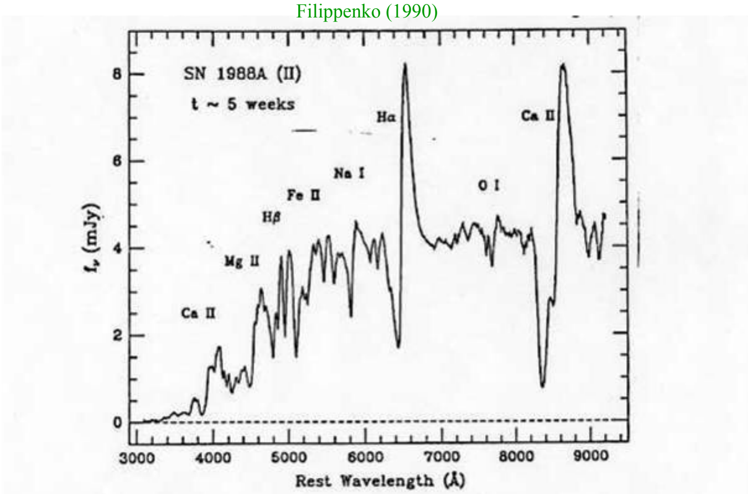

Figure 1: SN 1988A in M58, a typical SN II about 5 weeks past maximum brightness. Note the prominent P Cygni profiles, especially of Hα and the Ca II near-infrared triplet.

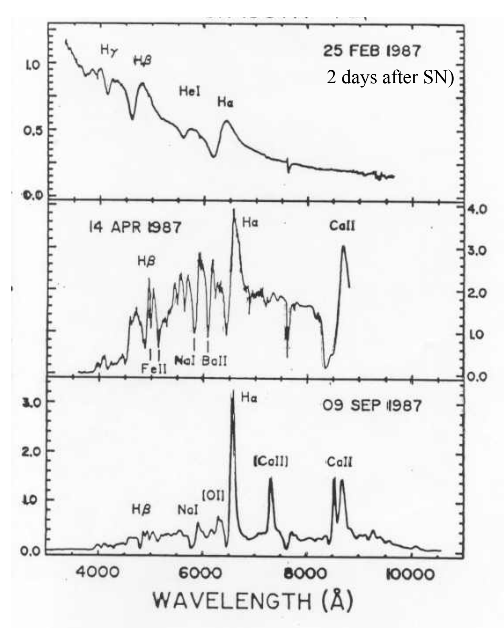

SN 1987A
Philipps (1987)
CTIO

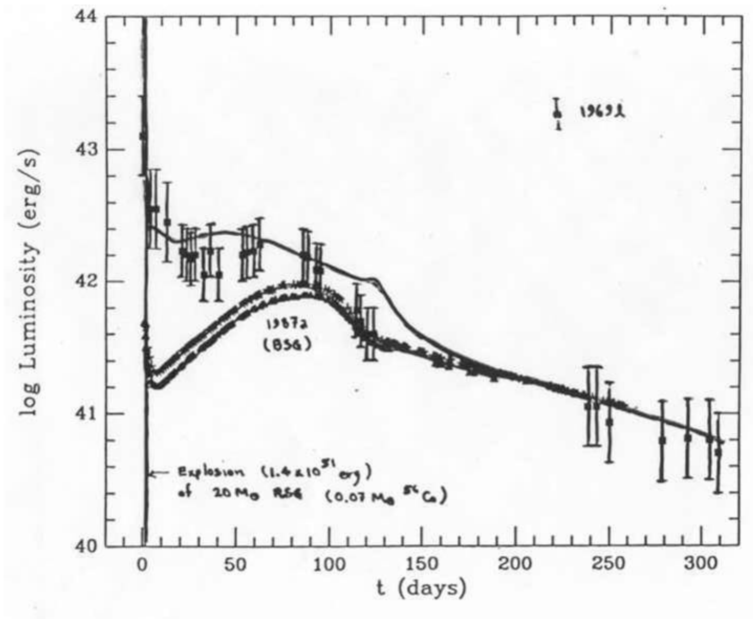

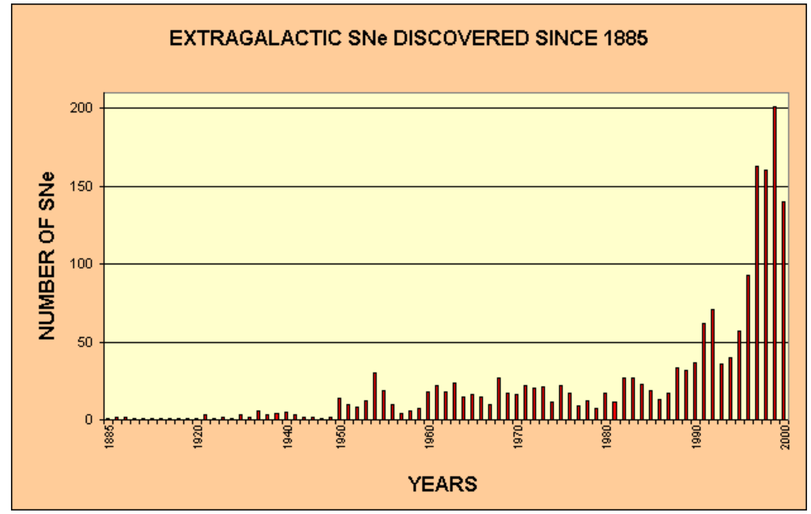

1952 supernovae were discovered in 2014.

Supernova Discovery Future

Rough predictions and promises…

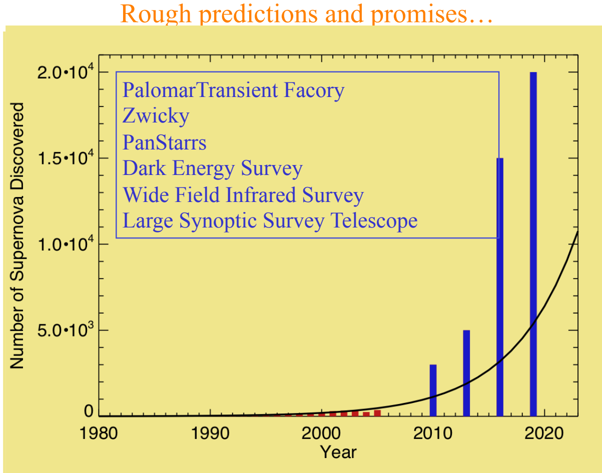

2010, statistics & trends

Project	Total SNe	Spec. confirmed	Mean redshift	Mean magnitude
CRTS	**189**	67 (35%)	0.057	18.0
PTF	**88**	88 (100%)	0.086	19.3
Amateurs	82	69 (84%)	0.019	16.7
PS1	63	63 (100%)	0.240	21.7
LOSS	50	48 (**96%**)	0.024	18.2
CHASE	36	32 (**89%**)	0.023	16.6
ROTSE	13	11 (85%)	0.051	17.9
LSSS	13	9 (69%)	0.033	17.4
MASTER	5	3 (60%)	0.034	16.2
Others	11	9 (82%)	-	-

Gal-Yam, Mazzali 2011 astro-ph 1103.5165

550 total (incomplete) – KAIT - 47

GAIA Distance Scale, Naples, May 5 2011

CTRS = Catalina Real Time Transient Survey

In a volume limited sample

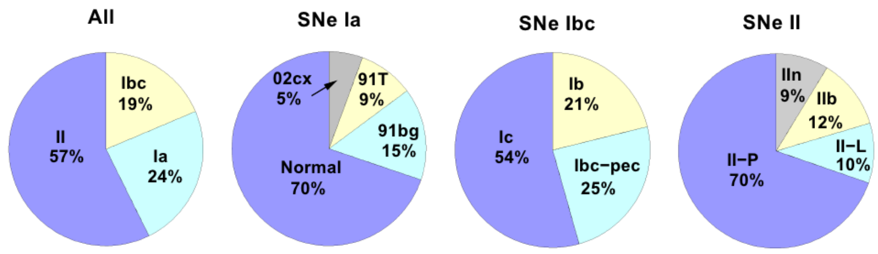

Li et al 2010, *MNRAS*, **412**, 1441

Tammann et al (1994) says total SN rate in MW is one every 40+-10 years, with 85% from massive stars. The very largest spirals produce about 10 SNae per century.

Good rule of thumb - 2 core collapse supernovae per centery; one SN Ia every other century

<u>Type II Supernovae</u>
Models and Physics of the Light Curve

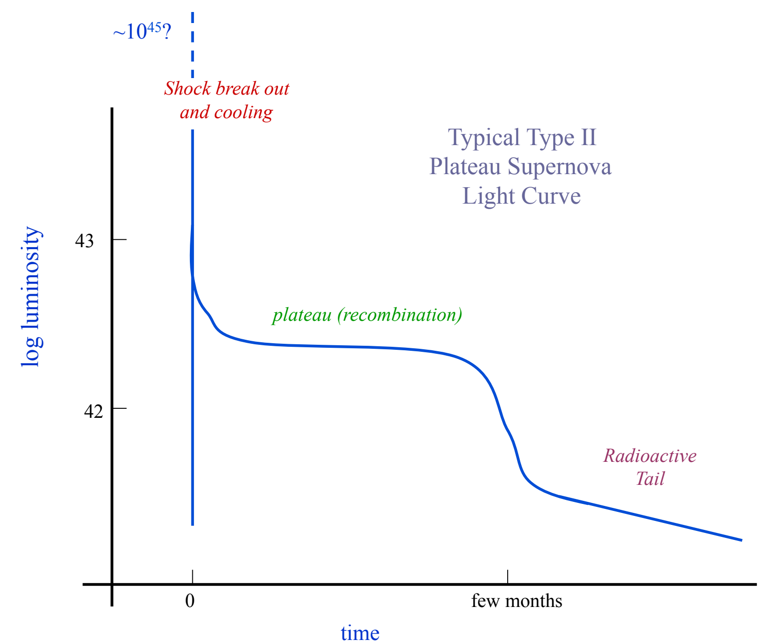

For a typical red supergiant derived from a star over 8 solar masses.

- *Break out – temperatures of 100's of thousands K. Very brief stage, not observed so far (indirectly in 87A). Shock heating followed by expansion and cooling*
- *Plateau – the hydrogen envelope expands and cools to ~5500 K. Radiation left by the shock is released. Nearly constant luminosity (T is constant and radius of photosphere does not change much – around 10^{15} cm). Lasts until the entire envelope recombines.*
- *Radioactive tail – powered by the decay of radioactive ^{56}Co produced in the explosion as ^{56}Ni.*

The light curve will vary depending upon the mass of the envelope, radius of the presupernova star, energy of the explosion, degree of mixing, and mass of ^{56}Ni produced.

Shock Break-out

1. *The electromagnetic display begins as the shock wave erupts through the surface of the star. A brief, hard ultra-violet (or even soft x-ray) transient ensues as a small amount of mass expands and cools very rapidly.*
   The transient is brighter and longer for larger progenitors but hotter for smaller ones

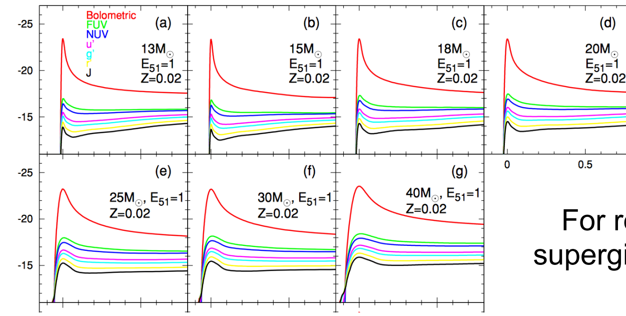

For red supergiants

Tominaga et al. 2011, *ApJ*, **193**, 20

Table 2
Properties of Shock Breakout

M_{MS} ($M_\odot$)	Z	E (10^{51} erg)	M_{ej} ($M_\odot$)	$T_{c,peak}$ (10^5 K)	$t_{1\,mag}$ (10^{-2} days)	$E_{rad,1\,mag}$ (10^{48} erg)	L_{peak} (10^{44} erg s^{-1})	$T_{c,peak}$ (10^5 K)	$t_{1\,mag}$ (10^{-2} days)	$E_{rad,1\,mag}$ (10^{48} erg)	L_{peak} (10^{44} erg s^{-1})
				Without Corrections					With Corrections		
13	0.02	1	11.2	3.56	0.651	0.691	10.3	3.35	1.09	0.815	6.99
15	0.02	1	12.7	3.68	0.512	0.536	10.2	3.48	0.915	0.643	6.64
18	0.02	1	15.2	3.03	0.994	0.948	9.41	2.87	1.46	1.09	6.90
20	0.02	1	16.8	2.80	1.19	1.11	9.11	2.70	1.68	1.26	6.91
25	0.02	1	19.9	2.17	2.94	2.07	6.78	2.04	3.40	2.23	5.99
30	0.02	1	23.0	1.99	3.51	2.39	6.52	1.87	3.97	2.54	5.86
40	0.02	1	19.6	2.01	5.16	4.57	8.55	1.92	5.60	4.82	7.90
25	0.02	4	19.8	3.23	1.27	4.20	32.5	3.08	2.28	5.05	21.1
25	0.02	10	19.7	4.38	0.763	6.83	89.6	3.96	2.12	8.74	42.4
25	0.02	20	19.6	5.21	0.511	10.0	196	4.88	2.06	13.5	72.4
20	0.001	1	17.9	2.57	1.35	0.896	6.51	2.51	1.77	1.01	5.23
20	0.004	1	17.8	2.91	1.09	0.986	8.80	2.76	1.54	1.12	6.64
20	0.05	1	15.7	2.41	2.14	1.80	8.09	2.31	2.64	1.99	6.88

Tominaga et al. 2011, *ApJ*, **193**, 20 0.01 d = 864 s

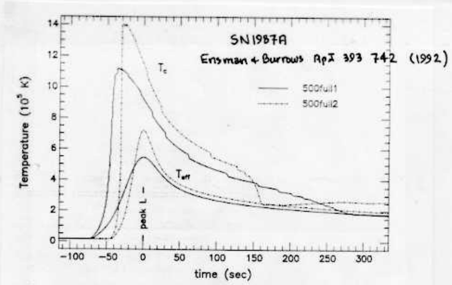

FIG. 11.—Color temperature and effective temperature of the emitted radiation as a function of time since peak luminosity for models 500full1 and 500full2. The top curve for each model is the color temperature, which is equal to the radiation temperature (and the gas temperature, except when the shock front passes through) at the thermalization depth. The small steps in the curves are numerical artifacts.

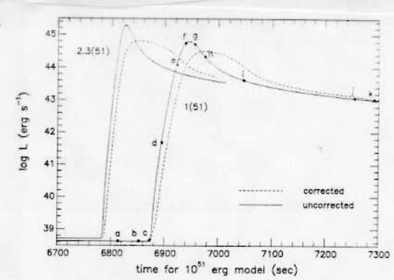

For SN 1987A detailed calculations exist. It was little hotter, briefer and fainter because it was a BSG with 10 times smaller radius than a RSG.

The effect of the uv-transient in SN 1987A was observed in the circumstellar ionization that it caused. The first spectroscopic observations of SN 1987A, made 35 hours after core collapse ($t = 0$ defined by the neutrino burst) – Kirshner et al, *ApJ*, **320**, 602, (1987), showed an emission temperature of 15,000 K that was already declining rapidly.

Ultraviolet observations later (Fransson et al, ApJ, 336, 429 (1989) showed *narrow* emission lines of N III, N IV, N V, and C III (all in the 1200 – 2000 Angstrom band). The ionization threshold for these species is 30 to 80 keV.

Modeling (Fransson and Lundquist *ApJL*, **341**, L59, (1989)) implied an irradiating flux with $T_e = 4$ to 8×10^5 K and an ionizing fluence (> 100 eV) ~ 2×10^{46} erg. This is in good agreement with the models.

The emission came from a circumstellar shell around the supernova that was ejected prior to the explosion – hence the narrow lines.

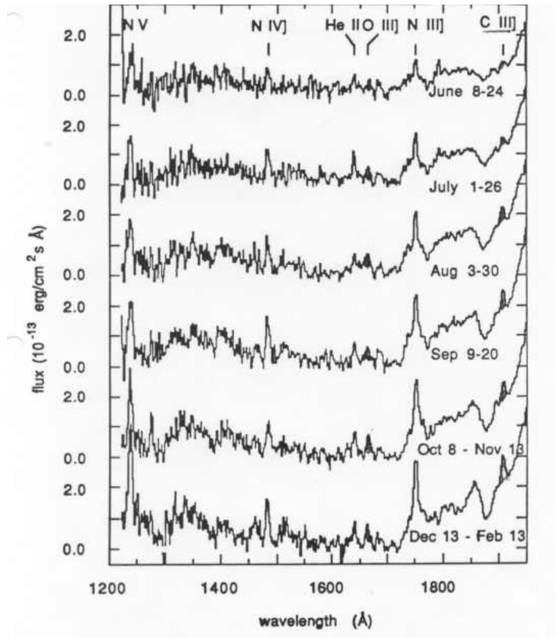

Fransson et al (1989)

IUE Observations of circumstellar material in SN 1987 A

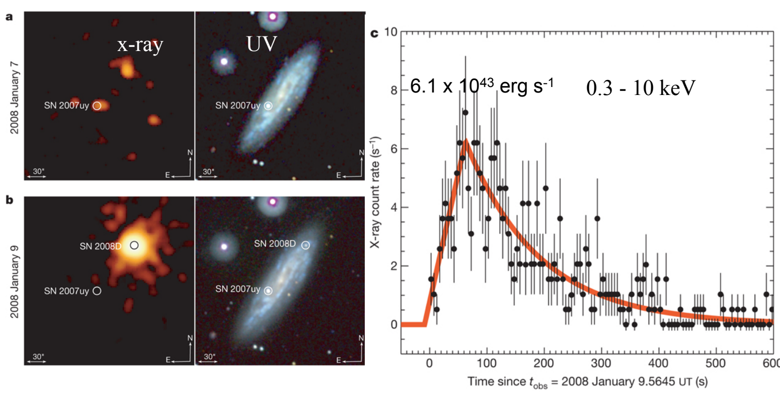

Soderberg et al 2008, *Nature*, **453**, 469

Shock breakout in Type Ib supernova SN 2008D (serendipitous discovery while observing SN 2007uy)

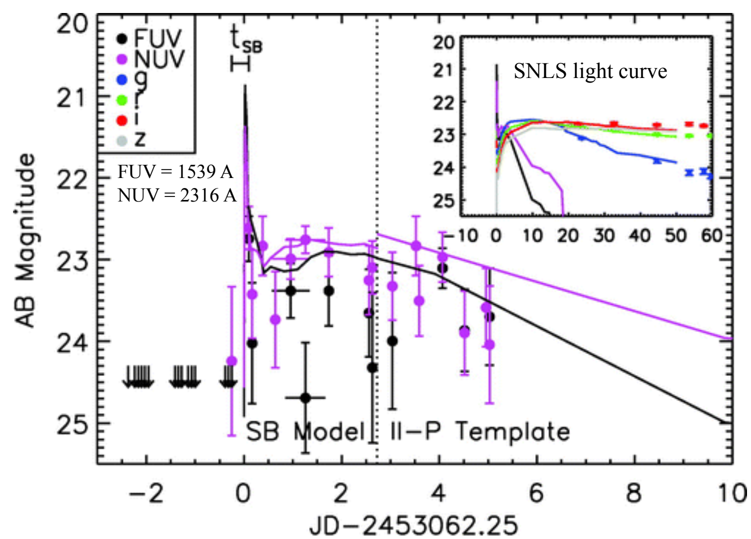

GALLEX discovery of ultraviolet emission just after shock break-out in a Type II-p supernova (Gezari et al 2008, ApJ, 683, L131). Missed the initial peak (about 2000 s, 90 Angstroms) but captured the 2 day uv-plateau

Modeling shows that they captured two supernovae, SNLS-04D2dc and SNLS-06D1jd within 7.1 hr and 13.7 hr after shock break out (in the SN rest frame)

SNLS = supernova legacy survey

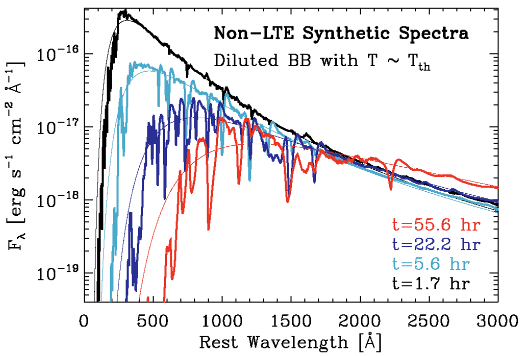

Kepler (15 Msun) plus CMFGEN models

2. <u>Envelope Recombination</u>

Over the next few days the temperature falls to ~5500 K, at which point, for the densities near the photosphere, hydrogen recombines. The recombination does not occur all at once for the entire envelope, but rather as a wave that propagates inwards in mass – though initially outwards in radius. During this time $R_{photo} \sim 10^{15} - 10^{16}$ *cm.*

The internal energy deposited by the shock is converted almost entirely to expansion kinetic energy. R has expanded by 100 or more (depending on the initial radius of the star) and the envelope has cooled dramatically.

$T \propto \frac{1}{r}$ $\qquad \rho \propto \frac{1}{r^3}$ $\qquad \rho \propto T^3$ (adiabatic with radiation entropy dominant)

$$\boxed{\varepsilon \propto \frac{T^4}{\rho} \propto \frac{1}{r}}$$

As a result only ~10^{49} *erg (RSG;* 10^{48} *BSG) is available to be radiated away. The remainder has gone into kinetic energy, now ~*10^{51} *erg.*

As the hydrogen recombines, the free electron density decreases and κ_{es} *similarly declines. (note analogy to the early universe)..*

H ionization - 15 solar masses. As the recombination front moves in the photospheric v declines. When the recombination reaches the He core the plateau ends

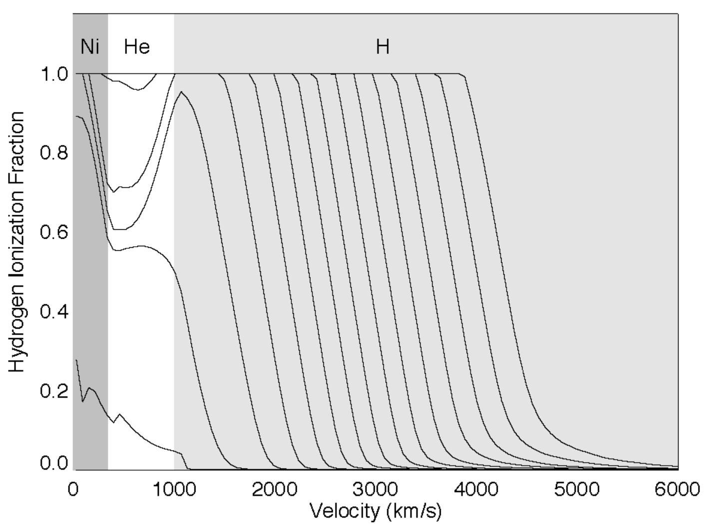

Photospheric speed

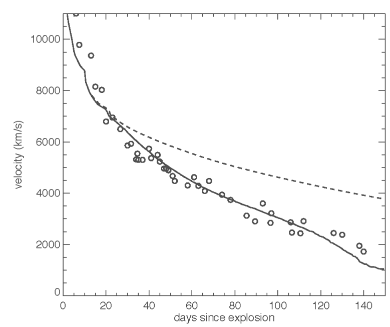

Kasen and Woosley (2009)

Fig. 4.— Photospheric velocity evolution of model M15_E1.2 as a function of time. The solid line shows the velocity of the electron scattering photosphere defined at $\tau_e = 2/3$. The dashed line shows the photospheric velocity in a model in which hydrogen recombination is neglected. The circles are the observed velocities of the sample of SNe IIP compiled by Nugent et al. (2006)

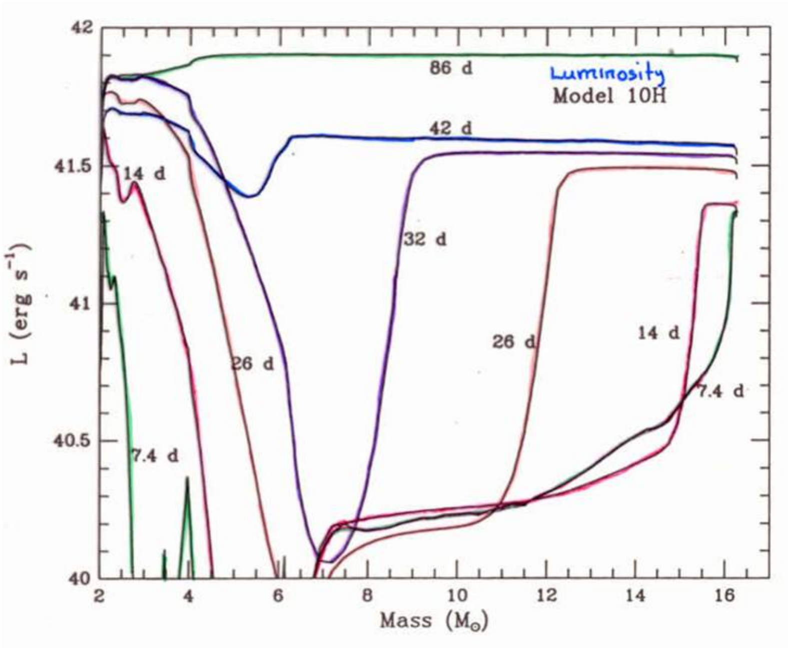

Popov (1993, *ApJ*, **414**, 712) gives the following scaling relations which he derives analytically:

$$t_{plateau} \approx 109\,\text{days}\,\frac{\kappa_{0.4}^{1/6}\,M_{10}^{1/2}\,R_{500}^{1/6}}{E_{51}^{1/6}\left(T_{ion}/4500\right)^{2/3}}$$

$$L_{bol} \approx 1.1\times10^{42}\,\frac{\text{erg}}{\text{s}}\,\frac{R_{500}^{2/3}\,E_{51}^{5/6}\left(T_{ion}/4500\right)^{4/3}}{M_{10}^{1/2}\,\kappa_{0.4}^{1/3}}$$

not quite linear in R because a more compact progenitor recombines at a slightly smaller radius.

where R_{500} is the radius of the preSN star in units of 500 R$_\odot$ (3.5×10^{13} cm);

$\kappa_{0.4}$ is the opacity in units of 0.4 cm^{2}gm^{-1}

M_{10} is the mass of the hydrogen envelope (not the star) in units of 10 M$_\odot$

E_{51} is the kinetic energy of the explosion in units of 10^{51} erg

T_{ion} is the recombination temperature (5500 is better than 4500)

In fact the correct duration of the plateau cannot be determined in a calculation that ignores radioactive energy input.

Cosmology on the Plateau
Baade-Wesselink Method
(akq "The Expanding Photosphere Method (EPM)

$$\phi = \frac{L}{4\pi D^2} = \frac{4\pi R_{ph}^2 \sigma T_e^4}{4\pi D^2} \qquad D = \text{distance}$$

$$D = R_{ph} T_e^2 \left(\frac{\sigma}{\phi}\right)^{1/2}$$

$$R_{ph} = R_{ph}^0 + v_{ph}(t - t_0)$$

can ignore R_{ph}^0

Measure on two or more occasions, t_i $- v_i, T_i,$ and ϕ_i

Solve for D and t_0.

In reality, the color temperature and effective temperature are not the same and that requires the solution of a model. But the physics of the plateau is well understood. This is a first principles method of getting distances. No Cepheid calibration is necessary - but it is helpful.

Eastman, Schmidt, and Kirshner (1996) give the dilution factor for a set of models

$H_0 = 73 \pm 7$

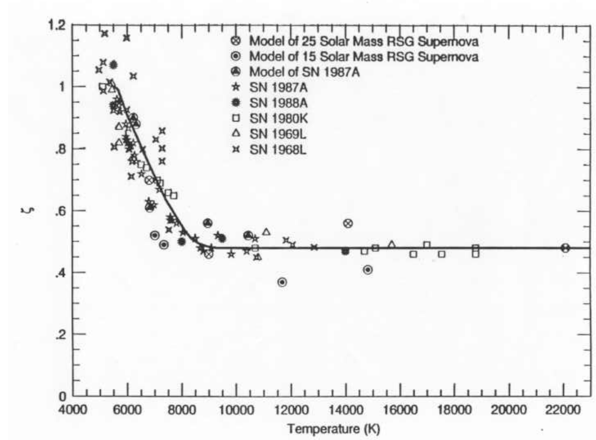

The dilution factor corrects for the difference between color temperature and effective temperature and also for the finite thickness of the photosphere which leads to a spread in T

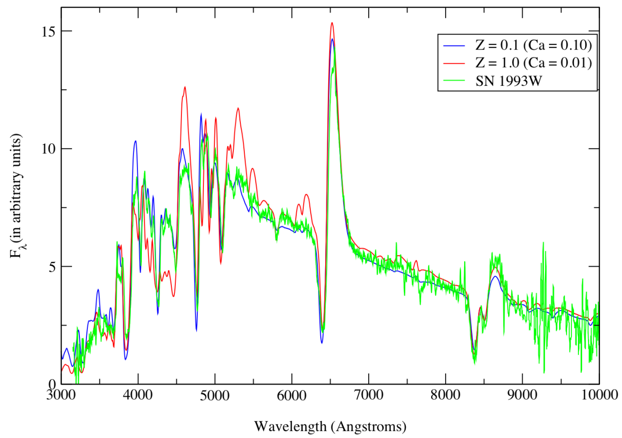

Modeling the spectrum of a Type II supernova in the Hubble flow (5400 km/s) by Baron et al. (2003). SN 1993W at 28 days. The spectrum suggests low metallicity. Sedonna code.

3. Light Curve Tail Powered by Radioactive Decay

a) $^{56}\mathrm{Ni}\,(e^-, \nu_e)\,^{56}\mathrm{Co}$ + 1.72 MeV in γ-rays

$\tau_{1/2} = 6.1$ d

$q_\gamma = 3.0 \times 10^{16}$ erg/gm

b) $^{56}\mathrm{Co}\,(e^-, \nu_e)\,^{56}\mathrm{Fe}$ 81%

and $(e^+ \bar{\nu}_e)\,^{56}\mathrm{Fe}$ 19% + 3.72 MeV in γ-rays

$\tau_{1/2} = 77.1$ d 6.4×10^{16} erg/gm

In 0.07 $M_\odot$ of $^{56}\mathrm{Ni} \rightarrow {}^{56}\mathrm{Fe}$ 1.3×10^{49} erg is released.

Implications for light curve and dynamics.

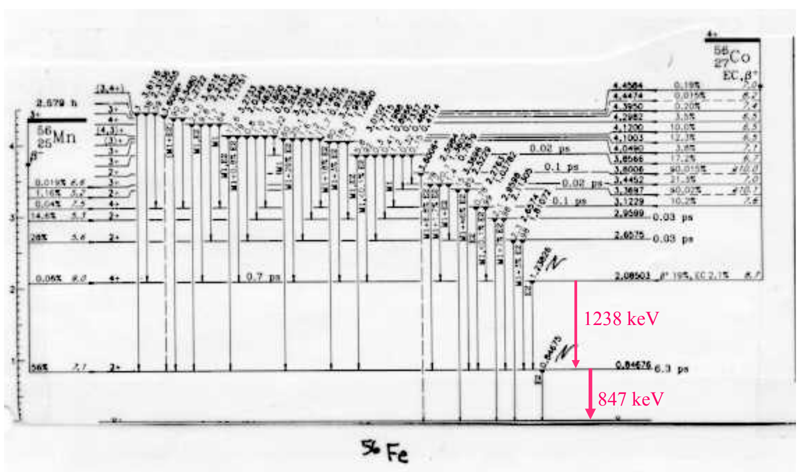

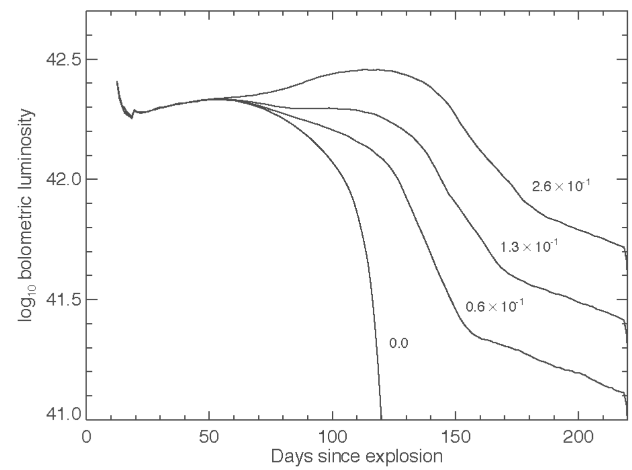

1.2 B explosion of 15 solar mass RSG with different productions of ^{56}Ni indicated by the labels. Kasen et al. (2009)

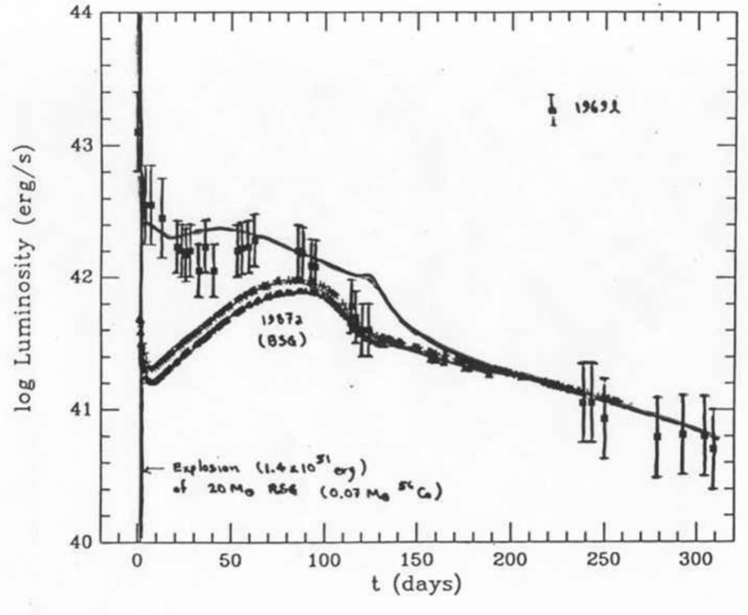

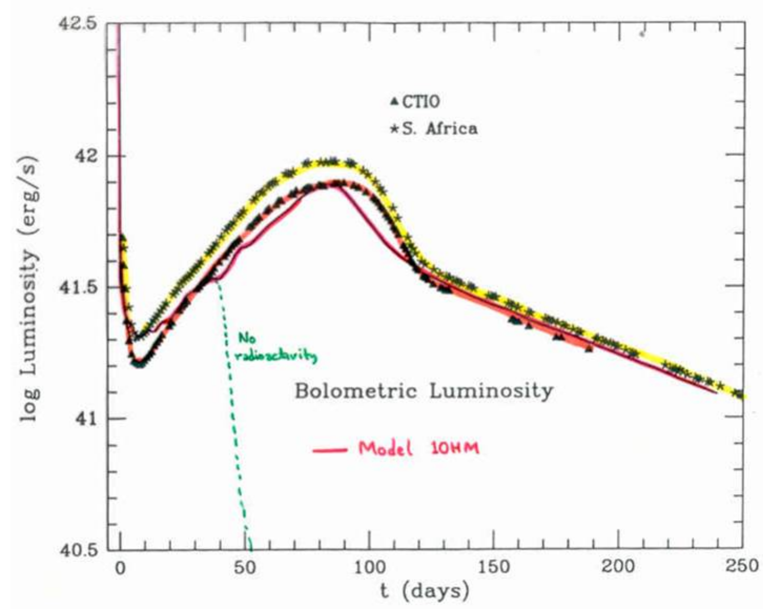

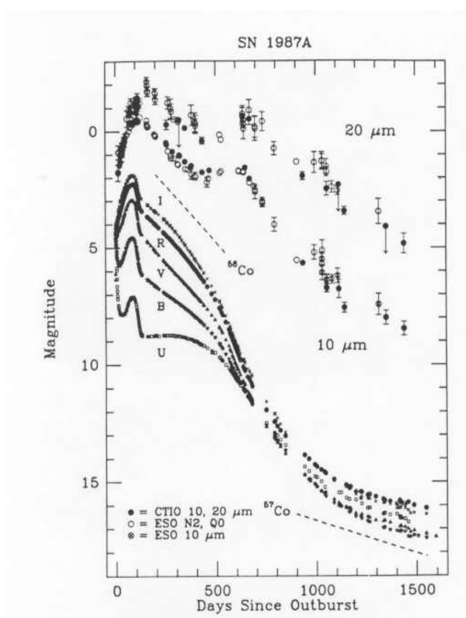

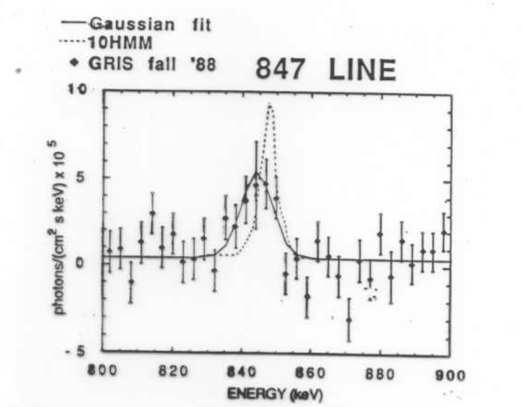

Figure 2. GRIS data for the 847 keV line from the decay of ^{56}Co in SN87A is shown for day 613. The top-of-atmosphere photon spectrum is shown in 3 keV bins which are larger than the FWHM resolution of the instrument. The solid line is a best fit to a Gaussian line profile. The dashed line is the predicted line profile for the 10HMM model. Although this model and similar spherically symmetric mixed models predict the line flux correctly there is a clear discrepancy with the measured line profile.

Other short lived radioactivites of interest:

$^{57}\mathrm{Co}(e^-,\bar{\nu}_e)^{57}\mathrm{Fe} \qquad \tau_{1/2} = 272$ days

$^{44}\mathrm{Ti}(e^-,\bar{\nu}_e)^{44}\mathrm{Sc} \qquad \tau_{1/2} = 60$ years

$^{44}\mathrm{Sc}(e^-,\bar{\nu}_e)^{44}\mathrm{Ca} \qquad = 2.44$ days

$^{44}\mathrm{Sc}(e^+\nu_e)^{44}\mathrm{Ca}$

The effect of ^{57}Co decay on the light curve of SN1987A was observed. ^{44}Ti hs been detected in both the Cas A SNR (Iyudin et al 1996) and SN1987A (Boggs et al, 2015).

The amount of ^{44}Ti seen in both cases was just over 10^{-4} $M_\odot$ which is a bit larger than most predictions. The motion also indicates assymetry in the explosion

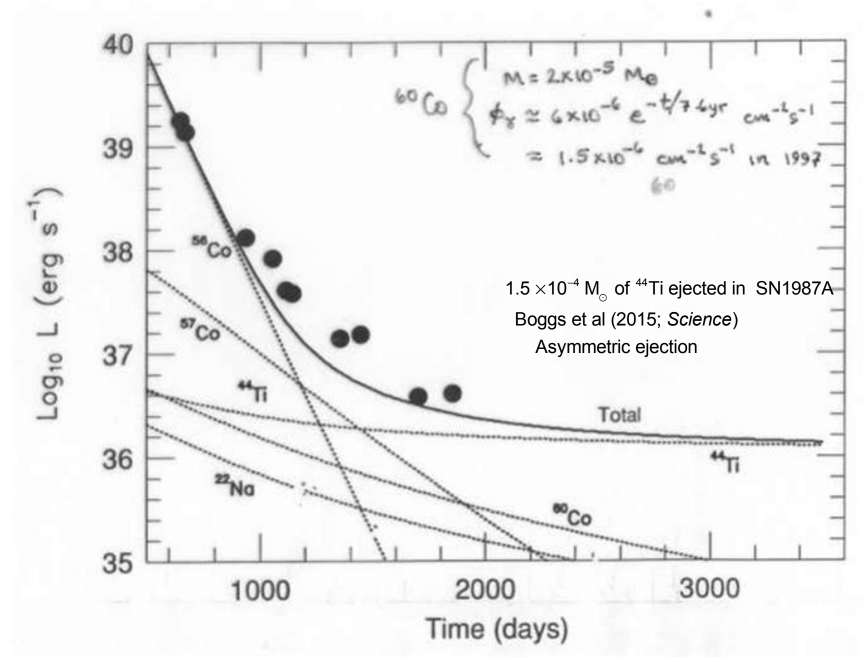

Exceptional Cases (models)

Faint supernovae

Stars in the ~8.5 – 10.5 solar mass range are virtually impossible not to explode, but the explosion energy will be low

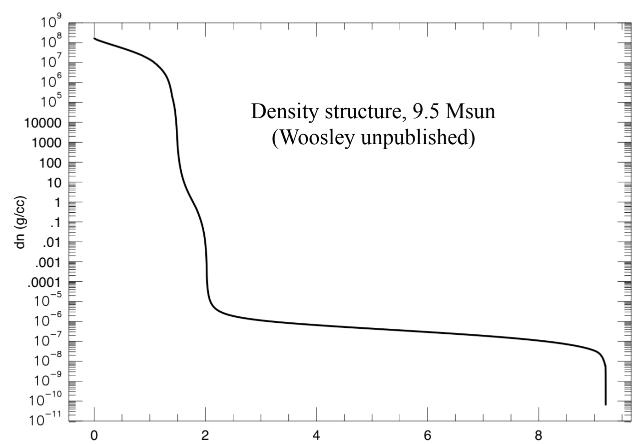

Energy of explosion given by (unavoidable) neutrino wind $\sim 10^{50}$ erg. 8 $M_\odot$ ejected so $v \sim 1000$ km s^{-1}

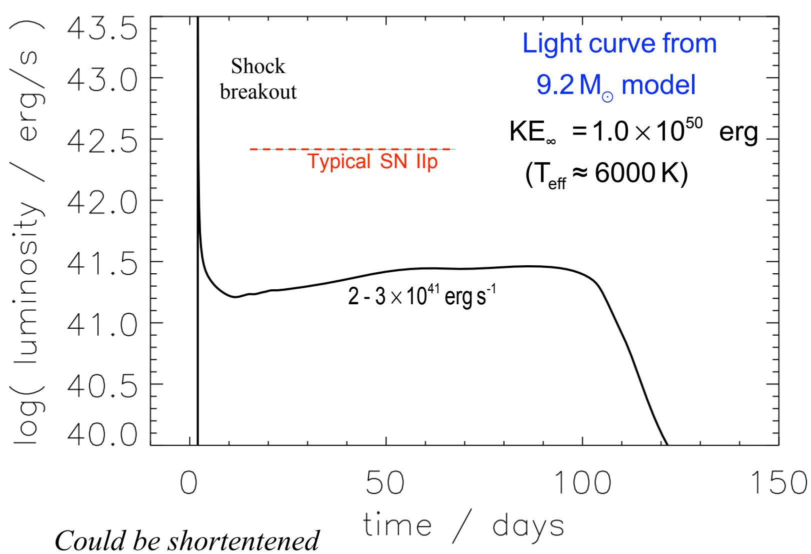

Could be shortentened by mass loss.

Magnetar illuminated supernovae:
(Woosley 2010, *ApJ*, **719**, 204)

- Approximately 10% of neutron stars are born as "magnetars", neutron stars with exceptionally high magnetic field strength (B ~ 10^{14-15} gauss) and possibly large rotation rates.
- A rotational period of 6 ms corresponds to 5 x 10^{50} erg. A high rotational rate may be required to make a magnetar. Where did this energy go?
- Moderate field strengths give a large late time energy input. In fact weaker fields can make brighter supernovae (for a given rotational energy). This reflects the competition between adiabatic energy loss and diffusion.

The initial explosion might not be rotationally powered but assume a highly magnetized pulsar is nevertheless created.

$$E_{51}(t=0) = 0.2\left(\frac{10\text{ ms}}{P_0}\right)^2$$

$$E_{51}(t) = \left(\frac{B_{15}^2\, t}{4\times 10^4} + \frac{1}{E_{51}(t=0)}\right)^{-1}$$

$$L = 10^{49}\ B_{15}^2 \left(\frac{E_{51}(t)}{20.}\right)^2 \propto \boxed{B_{15}^{-2}\ t^{-2}} \text{ at late times}$$

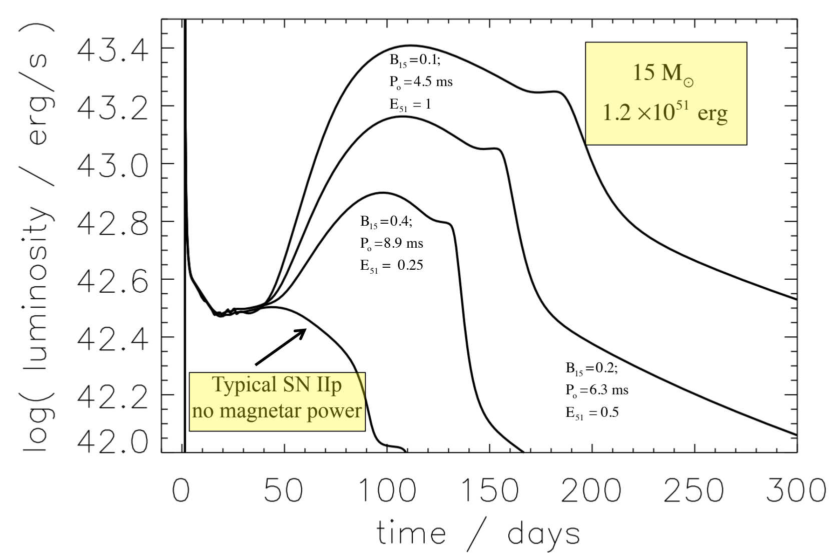

Maeda et al 2007; Woosley 2010; Kasen and Bildsten 2010

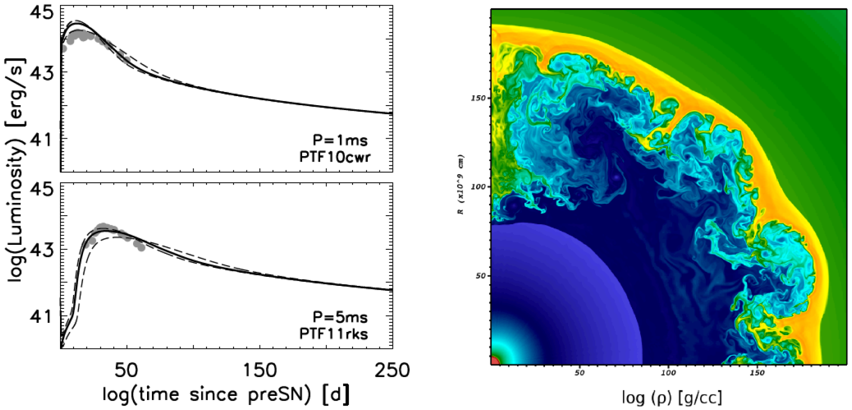

Chen, Woosley and Sukhbold – in prepration (2015)

and Type Ibc

The dashed line is for the decay of 0.3 solar masses of ^{56}Ni. Other lines are the calculated light curves for B_{15} = 0.5 and 0.7 and a neutron star rotational energy of 2 and 5 x 10^{50} erg.

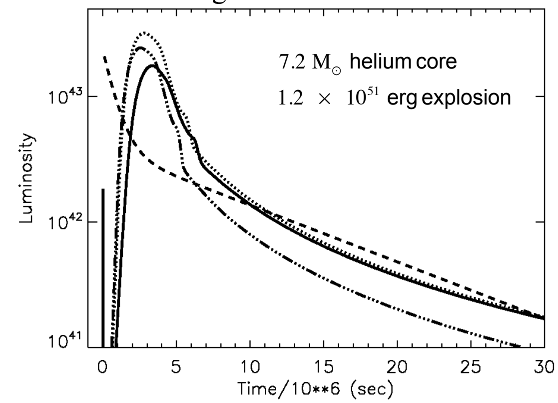

Woosley (2010)

TYPE Ib SUPERNOVAE

summary Porter & Filippenko (1987)

- Lack of 6150 Å Si II absorption trough
- Preference for galaxies of type Sbc or leter
- Proximity to H II regions
- Low luminosity w/r Type Ia (about -1.5 m)
- Distinct IR light curves having no secondary maximum about 1 mo after optical peak
- Reddish colors
- Radio emission within 1 year of explosion

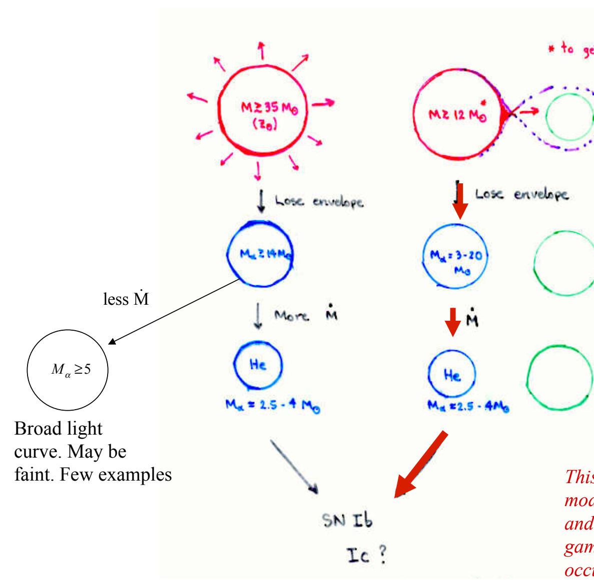

More recent studies suggest binary evolution the most likely path and $M_{\boxtimes}$ ~ 3 - 4 the most likely progenitor

This is for non-rotating models.For rapid rotation and high final mass gamma-ray bursts may occur

Recent Type Ib and Ic Simulations

f_{WR} is a reduction factor applied to older overly large WR mass loss rates

944 YOON, WOOSLEY, & LANGER Vol. 725

Table 1
Properties of the Computed Sequences

No.	Z	$M_{1,i}$	$M_{2,i}$	P_i	f_{WR}	Case	P_f	$M_{1,f}$	$M_{CO,f}$	M_{He}	M_H	$\langle j_{1.4} \rangle$	Fate
1	0.02	12	8	3.0	5	B+BB	57.9	1.40[a]	1.21[a]	0.17[a]	0.0	0.33	ONeMg WD
2	0.02	12	11	4.0	5	B+BB	104.4	1.48[a]	1.24[a]	0.20[a]	0.0	0.35	ONeMg WD
3	0.02	13	11	5.0	5	B+BB	123.3	1.64[a]	1.43[a]	0.18[a]	0.0	0.22	SN Ic
4	0.02	14	12	3.0	5	A+AB+BB	118.5	1.33[a]	1.09[a]	0.22[a]	0.0	···	ONeMg WD
5	0.02	14	12	5.0	5	B+BB	30.7	2.97	1.66	1.24	1.9(−4)	0.25	SNIb
6	0.02	16	14	2.0	5	A:Contact							
7	0.02	16	14	3.0	5	A+AB+ABB	101.8	1.54[a]	1.33[a]	0.17[a]	0.0	0.39	ONeMg WD
8	0.02	16	14	4.0	5	B+BB	26.2	3.66	2.05	1.47	4.5(−3)	0.24	SNIb
9	0.02	16	14	5.0	5	B+BB	33.7	3.65	2.04	1.47	5.0(−3)	0.25	SNIb
10	0.02	18	12	3.0	5	A+AB+ABB	27.9	2.66	1.58	1.01	0.00	0.26	SNIb
11	0.02	18	12	3.0	10	A+AB+ABB	27.3	2.74	1.59	1.08	0.00	0.26	SNIb
12	0.02	18	12	5.0	10	B:Contact							
13	0.02	18	17	3.0	10	A+AB+ABB	36.2	3.03	1.68	1.27	7.9(−4)	0.25	SN Ib
14	0.02	18	17	4.0	10	A+AB	29.7	3.79	2.14	1.49	1.5(−3)	0.25	SN Ib
15[b]	0.02	18	17	4.0	10	A+AB	24.0	3.97	2.27	1.53	1.0(−3)	0.26	SNIb
16[c]	0.02	18	17	4.0	10	A+AB	50.0	3.80	2.16	1.50	2.2(−3)	0.06	SNIb
17[d]	0.02	18	17	4.0	10	A+AB	25.2	3.84	2.18	1.50	1.4(−3)	0.26	SNIb
18[e]	0.02	18	17	4.0	10	A+AB	30.6	3.73	2.14	1.43	0.00	3.57	SNIb
19	0.02	18	17	5.0	3	B	33.1	3.73	2.33	1.23	0.00	0.25	SNIb
20	0.02	18	17	5.0	5	B	32.4	4.04	2.45	1.4	0.00	0.33	SNIb
21	0.02	18	17	5.0	10	B+BB	31.5	4.41	2.51	1.68	9.9(−3)	0.26	SNIb
22	0.02	18	17	6.0	10	B	39.3	4.39	2.56	1.62	4.0(−3)	0.26	SNIb
23	0.02	25	19	6.0	10	B:Contact							
24	0.02	25	24	2.0	10	A:Contact							
25	0.02	25	24	3.0	3	A+AB	22.7	3.70	2.46	0.98	0.0	0.24	SNIb
26	0.02	25	24	3.0	5	A+AB	22.4	4.33	2.80	1.30	0.0	0.25	SNIb
27	0.02	25	24	3.0	10	A+AB	21.3	5.07	3.17	1.67	0.0	0.25	SNIb
28[d]	0.02	25	24	3.0	10	A+AB	18.9	5.08	3.19	1.66	0.0	0.32	SNIb
29	0.02	25	24	4.0	5	A + AB	21.5	4.45	2.91	1.22	0.0	0.26	SNIb
30	0.02	25	24	6.0	10	B	27.4	6.49	4.45	1.63	0.0	0.39	SNIb
31	0.02	60	40	7.0	3	A	16.8	4.95	3.70	0.25	0	0.24	SNIc
32	0.004	16	12	3.0	5	B+BB	64.75	3.91	2.22	1.54	1.6(−2)	0.24	SNIb
33	0.004	16	14	3.0	5	B+BB	19.6	3.90	2.21	1.53	1.6(−2)	0.24	SNIb
34	0.004	16	14	5.0	5	B+BB	21.8	3.84	2.19	1.51	1.2(−2)	0.24	SNIb
35	0.004	18	12	5.0	5	B+BB	14.4	4.64	2.76	1.68	1.7(−2)	0.31	SNIb
36	0.004	18	12	8.0	5	B+BB	24.33	4.56	2.68	1.67	1.5(−2)	0.33	SNIb
37	0.004	18	17	3.0	5	A+AB	18.4	4.42	2.55	1.67	2.6(−2)	0.26	SNIb
38	0.004	18	17	3.0	10	A+AB	14.4	4.58	2.61	1.77	2.7(−2)	0.26	SNIb
39	0.004	18	17	6.0	5	B+BB	27.0	4.57	2.71	1.65	1.6(−2)	0.27	SNIb
40	0.004	25	12	3.0	5	A:Contact							
41	0.004	25	12	6.0	5	B:Contact							
42	0.004	25	19	3.0	5	A+AB	10.2	7.09	4.87	2.03	6.5(−3)	0.32	SNIb
43	0.004	25	24	3.0	5	A+AB	13.0	7.31	5.05	2.07	8.7(−3)	0.28	SNIb
44	0.004	25	24	6.0	5	B:Contact							
45	0.004	40	30	4.0	5	A+AB	9.31	12.0	9.42	1.24	0.0	0.56	BH

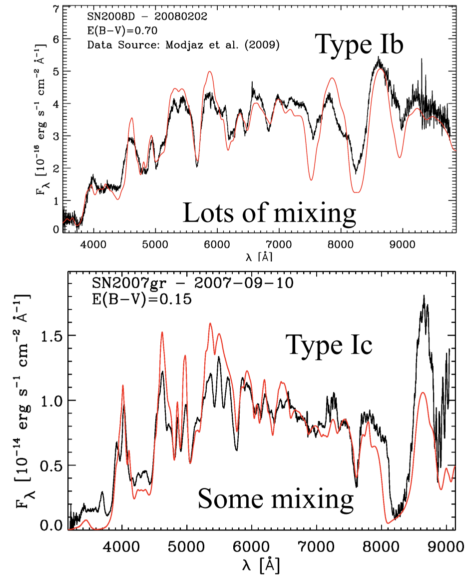

Dessart, Hillier, & Woosley, MNRAS, 424, 2139 (2012)

It is popular (mis)conception that the production of Type Ic supernovae requires the removal of the hydrogen envelope and helium shell of a very massive star in order to have a weak helium line at 5876 A.

The two models on the left are both derived from a 5.1 helium star that originated from a binary pair in which each star was lighter than 20 solar masses (Yoon, Langer and Woosley 2010)

2156 *L. Dessart et al.*